409. Dynamical directivity and chaos in some systems with supplementary degrees of freedom

K. Ragulskis
Lithuanian Academy of Sciences, Kaunas, Lithuania
e-mail: kazimieras3@hotmail.com, kazimieras3@yahoo.com
Phone/Fax: +370 37 796724

(Received:20 October; accepted: 02 December)

Abstract.

In systems with supplementary degrees of freedom dynamical directivity followed by chaos may exist. Deterministic systems of such types are analyzed in the paper. Their steady state regimes which take place according to dynamically self setting trajectories or vibration modes depending on the eigenfrequencies of the system itself and on the excitation frequencies and parameters are determined. The research is performed by applying approximate analytical methods and numerical ones.

Keywords: dynamical directivity, trajectories and modes of motion, stability, chaos.

Introduction

Dynamical directivity is the quality of a definite type of nonlinear dynamical systems having supplementary degrees of freedom to choose its structure or laws of motion or trajectories depending on the parameters of the system itself and of the forces excited by it [3]. This research paper is one of the investigations of the effect of self-organization [1, 2]. Theory of stability and chaos are developed in a number of research publications [4 – 12 and others], which were useful in the process of preparation of this paper.

Here dynamical directivity of deterministic systems is analyzed:

1. the simplest system,
2. system with concentrated parameters,
3. system with distributed parameters.

The research is performed approximately analytically by using the method of perturbation, by numerical methods and experimentally.

1. The elementary system

The case 1 of the input member – the exciter of vibrations is attached to the output member 2 by a hinge joint. The mass 3 exciting the vibrations moves in the line *AB*. The output member is supporting to the immovable plane *XOY*. Viscous friction with coefficients H_x and H_y respectively according to the axes *OX* and *OY* is acting between them. The mass 3 is moving according to the law $z = AB = A\cos\omega t$. The external force $P = const$ is acting to the case of the exciter of vibrations at the point *A*. The system is moving with the velocity $\dot{s}$.

Coordinates of the points are $A(x, y)$, $B(x + z\cos\alpha, y + z\sin\alpha)$.

Kinetic energy and the dissipative function of the system:

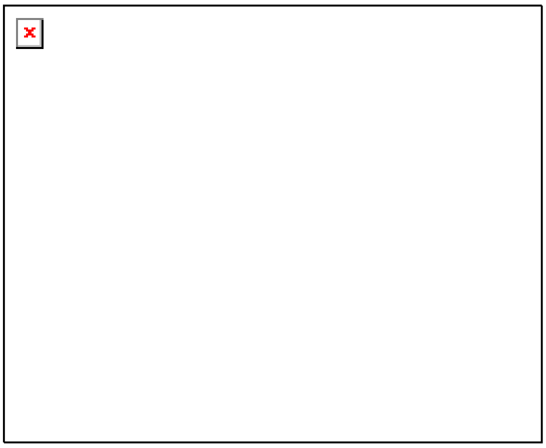

Fig. 1. The elementary system: 1 – input member, 2 – output member, 3 – mass exciting vibrations

$$2T = m_x\dot{x}^2 + m_y\dot{y}^2 + \\ + m\begin{bmatrix} \dot{z}^2 + z^2\dot{\alpha}^2 + \\ + 2\dot{x}(\dot{z}\cos\alpha - z\dot{\alpha}\sin\alpha) + \\ + 2\dot{y}(\dot{z}\sin\alpha + z\dot{\alpha}\cos\alpha) \end{bmatrix} + J\dot{\alpha}^2,$$

$$2D = H_x \dot{x}^2 + H_y \dot{y}^2 + H_\alpha \dot{\alpha}^2. \tag{1}$$

Differential equations of motion:

$$\begin{aligned} &M_i(\alpha) + H_\alpha \dot{\alpha} = 0, \\ &I_i(x) + H_x \dot{x} = P\cos(\beta+\alpha), \\ &I_i(y) + H_y \dot{y} = P\sin(\beta+\alpha), \end{aligned} \tag{2}$$

where the influence of the forces of inertia to the coordinates α, x, y respectively:

$$\begin{aligned} &M_i(\alpha) = I\ddot{\alpha} + mz(z\ddot{\alpha} + 2\dot{z}\dot{\alpha} - \ddot{x}\sin\alpha + \ddot{y}\cos\alpha), \\ &I_i(x) = m_x\ddot{x} + \\ &+ m\left[\left(\ddot{z} - z\dot{\alpha}^2\right)\cos\alpha - \left(z\ddot{\alpha} + 2\dot{z}\dot{\alpha}\right)\sin\alpha\right], \\ &I_i(y) = m_y\ddot{y} + \\ &+ m\left[\left(\ddot{z} - z\dot{\alpha}^2\right)\sin\alpha + \left(z\ddot{\alpha} + 2\dot{z}\dot{\alpha}\right)\cos\alpha\right]. \end{aligned} \tag{3}$$

In quasi-linear case steady state motions are:

$$\begin{aligned} &\alpha_0 = const, \\ &x_0 = \frac{P}{H_x} t\cos(\beta+\alpha) + \\ &+ \frac{\mu_x \omega A\cos\alpha_0}{\omega^2 + h_x^2}\left(-\omega\cos\omega t + h_x\sin\omega t\right), \\ &y_0 = \frac{P}{H_y} t\sin(\beta+\alpha) + \\ &+ \frac{\mu_y \omega A\sin\alpha_0}{\omega^2 + h_y^2}\left(-\omega\cos\omega t + h_y\sin\omega t\right), \end{aligned} \tag{4}$$

$$\mu_x = \frac{m}{m_x}, \ \mu_y = \frac{m}{m_y}, \ h_x = \frac{H_x}{m_x}, \ h_y = \frac{H_y}{m_y}.$$

In the case of steady state motions:

$$\begin{aligned} &\overline{M_i(\alpha)} \equiv \\ &\equiv \left[\omega^2\left(\mu_y - \mu_x\right) + \mu_y h_x - \mu_x h_y\right]\sin 2\alpha_0 = 0, \end{aligned} \tag{5}$$

from here in the case when:

$$\left[\omega^2\left(\mu_y - \mu_x\right) + \mu_y h_x - \mu_x h_y\right] > 0,$$

$\alpha_0 = 0$ is a stable regime,

$\alpha_0 = \dfrac{\pi}{2}$ is an unstable regime. (6)

When the sign of the inequality is the opposite the stable and unstable regimes change into the opposite ones.

The average velocity is as follows:

$$\vec{\dot{s}} = \vec{\dot{s}}_x + \vec{\dot{s}}_y,$$

and the angle of its direction:

$$tg\gamma = \frac{\dfrac{m_y}{m_x}}{1 + \dfrac{H_x}{H_y} tg(\beta + \alpha_0)}. \tag{7}$$

2. System with concentrated parameters

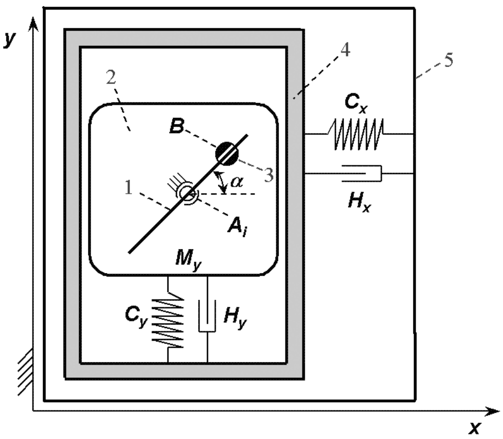

Fig. 2. The system: 1 – input member, 2 – output member, 3 – mass exciting vibrations, 4 and 5 – directing members

In the same way as in Fig. 1 the input member – the case 1 of the exciter of vibrations is attached by a hinge to the output member 2. The mass 3 exciting vibrations is moving along the line *AB*. The output member supports to the immovable plane *XOY*. Viscous friction with the coefficients H_{x0} and H_{y0} respectively according to the coordinates *OX* and *OY* is acting between them.

Mass 3 is moving according to the law $z = AB\cos\omega t = A\cos\omega t.$ External force $P = const$ is acting to the case of the exciter of vibrations at the point *A*. The system is moving with the velocity $\dot{s}$. Member 2 is connected with the member 4 by an elastic dissipative element with the coefficients H_y and C_y, and member 4 is connected with the member 5 by an element with the coefficients H_x and C_x.

Kinetic and potential energies of the system and the dissipative function are:

$$\begin{aligned} &2T = m_x\dot{x}^2 + m_y\dot{y}^2 + \\ &+ m\begin{bmatrix} \dot{z}^2 + z^2\dot{\alpha}^2 + \\ + 2\dot{x}(\dot{z}\cos\alpha - z\dot{\alpha}\sin\alpha) + \\ + 2\dot{y}(\dot{z}\sin\alpha + z\dot{\alpha}\cos\alpha) \end{bmatrix} + \\ &+ m_5\dot{x}_5^2 + m_{y4}\dot{y}_4^2 + J\dot{\varphi}^2, \\ &2\Pi = C_x\left(x - x_5\right)^2 + C_y\left(y - y_4\right)^2, \\ &2D = H_x\left(\dot{x} - \dot{x}_5\right)^2 + H_y\left(\dot{y} - \dot{y}_4\right)^2 + \\ &+ H_{x0}\dot{x}^2 + H_{y0}\dot{y}^2 + H_\alpha\dot{\alpha}^2, \end{aligned} \tag{8}$$

Where:

$$m_x = m_1 + m_2 + m + m_4, \qquad m_y = m_1 + m_2 + m,$$
$$m_3 = m, \ m_{y4} = m_4 + m_5.$$

Differential equations of motion of the system are expressed in the following way:

$$
\begin{aligned}
& M_i(\alpha)+H_\alpha\dot{\alpha}=0, \\
& I_i(x)+C_x(x-x_5)+H_x(\dot{x}-\dot{x}_5)+H_{x0}\ddot{x}= \\
& =P\cos(\beta+\alpha), \\
& I_i(y)+C_y(y-y_4)+H_y(\dot{y}-\dot{y}_4)+H_{y0}\dot{y}= \\
& =P\sin(\beta+\alpha), \\
& m_{y4}\ddot{y}_4+C_y(y_4-y)+H_y(\dot{y}_4-\dot{y})=0, \\
& m_5\ddot{x}_5+C_x(x_5-x)+H_x(\dot{x}_5-\dot{x})=0,
\end{aligned}
\tag{9}
$$

where $M_i(\alpha)$, $I_i(x)$, $I_i(y)$ are determined from the equations (2).

After introducing the notation:

$$
I\ddot{\alpha}+
+\varepsilon\left[mz\begin{pmatrix} z\ddot{\alpha}+2\dot{z}\dot{\alpha}- \\ -\ddot{x}\sin\alpha+\ddot{y}\cos\alpha \end{pmatrix}+H_\alpha\dot{\alpha}\right]=0,
\tag{10}
$$

where ε – a small parameter, steady state motions according to α, x, y, y_4, x_5 are sought with the help of power series with respect to ε, for example $\alpha=\alpha_0+\varepsilon\alpha_1+\ldots$.

After introducing the notations:

$$
\begin{aligned}
& \mu_x=\frac{m}{m_x},\quad n_x^2=\frac{C_x}{m_x},\quad h_x=\frac{H_x}{m_x},\quad h_{x0}=\frac{H_{x0}}{m_x}, \\
& P_x=\frac{P}{m_x},\quad \mu_y=\frac{m}{m_y},\quad n_y^2=\frac{C_y}{m_y},\quad h_y=\frac{H_y}{m_y}, \\
& h_{y0}=\frac{H_{y0}}{m_y},\quad P_y=\frac{P}{m_y},\quad n_5^2=\frac{C_x}{m_5},\quad h_5=\frac{H_5}{m_5}, \\
& n_4^2=\frac{C_y}{m_{y4}},\ h_4=\frac{H_y}{m_4},
\end{aligned}
\tag{11}
$$

equations of zero approximation are the following ones:

$$
\begin{aligned}
& \ddot{\alpha}_0=0,\ \alpha_0=const, \\
& \ddot{x}_0+\mu_x\ddot{z}\cos\alpha_0+n_x^2(x_0-x_{50})+ \\
& +h_x(\dot{x}_0-\dot{x}_{50})+h_{x0}\dot{x}_0=P_x\cos(\beta+\alpha), \\
& \ddot{y}_0+\mu_y\ddot{z}\cos\alpha_0+n_y^2(y_0-y_{40})+ \\
& +h_y(\dot{y}_0-\dot{y}_{40})+h_{y0}\dot{y}_0=P_y\sin(\beta+\alpha), \\
& \ddot{x}_{50}+n_5^2(x_{50}-x_0)+h_5(\dot{x}_{50}-\dot{x}_0)=0, \\
& \ddot{y}_{40}+n_4^2(y_{40}-y_0)+h_4(\dot{y}_{40}-\dot{y}_0)=0.
\end{aligned}
\tag{12}
$$

From the equations (12), when $H_x=H_y=0$, the following is obtained:

$$
\begin{aligned}
& x_0=\mu_x\omega A\cos\alpha_0\frac{(\omega^2-n_5^2)^2}{\lambda_x^2\omega^2+h_{x0}^2(\omega^2-n_5^2)^2}\cdot \\
& \cdot\left(-\frac{\lambda_x}{\omega^2-n_5^2}\omega\cos\omega t+h_{x0}\sin\omega t\right)+ \\
& +\frac{P_x\cos(\beta+\alpha_0)}{h_{x0}}t, \\
& y_0=\mu_y\omega A\sin\alpha_0\frac{(\omega^2-n_4^2)^2}{\lambda_y^2\omega^2+h_{y0}^2(\omega^2-n_4^2)^2}\cdot \\
& \cdot\left(-\frac{\lambda_y}{\omega^2-n_4^2}\omega\cos\omega t+h_{x0}\sin\omega t\right)+ \\
& +\frac{P_y\sin(\beta+\alpha_0)}{h_{y0}}t,
\end{aligned}
\tag{13}
$$

where it is denoted:

$\lambda_x=\omega^2-(n_x^2+n_5^2)$, $\lambda_y=\omega^2-(n_y^2+n_4^2)$.

The condition of periodicity of α_1 on the basis of equation (10) is:

$$
\Lambda=\int_t^{t+\frac{2\pi}{\omega}}\left[mz\begin{pmatrix} z\ddot{\alpha}_0+2\dot{z}\dot{\alpha}_0- \\ -\ddot{x}_0\sin\alpha_0+ \\ +\ddot{y}_0\cos\alpha_0 \end{pmatrix}+ \atop +H_\alpha\dot{\alpha}_0\right]dt=0,
\tag{14}
$$

which after rearrangements becomes the following one:

$$
\Lambda=Z\sin 2\alpha_0=0,
\tag{15}
$$

Where

$$
Z=
=\frac{0{,}25(\omega^2 A)^2}{\begin{bmatrix}\lambda_x^2\omega^2+ \\ +h_{x0}^2(\omega^2-n_5^2)^2\end{bmatrix}\begin{bmatrix}\lambda_y^2\omega^2+ \\ +h_{y0}^2(\omega^2-n_4^2)^2\end{bmatrix}}Z_s,
\tag{16}
$$

where the sign change of Z depending on ω^2 is determined by:

$$
\begin{aligned}
& Z_s=\omega^2\lambda_x\lambda_y(\omega^2-\omega_{k1}^2)(\omega^2-\omega_{k2}^2)+ \\
& +\begin{bmatrix}-\mu_x h_y^2\lambda_x(\omega^2-n_4^2)+ \\ +\mu_y h_x^2\lambda_y(\omega^2-n_5^2)\end{bmatrix}\cdot \\
& \cdot(\omega^2-n_4^2)(\omega^2-n_5^2).
\end{aligned}
\tag{17}
$$

ω_{k1}^2 and ω_{k2}^2 are the roots of the following equation:

$$a_4\omega^4 + a_2\omega^2 + a_0 = 0, \tag{18}$$

Where:

$$a_4 = -\mu_x + \mu_y,$$

$$a_2 = \mu_x\left(n_y^2 + n_4^2 + n_5^2\right) - \mu_y\left(n_x^2 + n_4^2 + n_5^2\right),$$

$$a_0 = -\mu_x\left(n_y^2 + n_4^2\right)n_5^2 + \mu_y\left(n_x^2 + n_5^2\right)n_4^2.$$

Dynamical stationary positions according to the equation (15) are:

$$\alpha_0 = 0, \frac{\pi}{2}, \tag{19}$$

and the condition of stability is:

$$Z\cos 2\alpha_0 > 0. \tag{20}$$

As follows from the equation (17) Z_S according to ω^2 may change sign at:

$$\omega_1^2 = n_x^2 + n_5^2, \qquad \omega_2^2 = n_y^2 + n_4^2, \qquad \omega_3^2 = \omega_{k1}^2,$$

$$\omega_4^2 = \omega_{k2}^2, \tag{21}$$

when $h_{x0} = h_{y0} = 0$. If $h_{x0} \neq 0$, $h_{y0} \neq 0$ then those values ω_i^2 $(i = 1, \ldots, 4)$ move to the sides from the values shown in the equations (21).

Case study:

$$y_4 = x_5 = h_{x0} = h_{y0} = 0, \tag{22}$$

by taking into account the equations (8 - 11) the following differential equations are obtained:

$$\begin{aligned} &\ddot{x}_i + h_x\dot{x}_i + p_x^2 x_i = X_i;\\ &\ddot{y}_i + h_y\dot{y}_i + p_y^2 y_i = Y_i;\\ &J\ddot{\alpha} + H_\alpha\dot{\alpha} = L, \end{aligned} \tag{23}$$

Where:

$$\begin{aligned} &X_i =\\ &= -\mu_x\left(\left(\ddot{z} - z\dot{\alpha}^2\right)\cos\alpha - \left(z\ddot{\alpha} + 2\dot{z}\dot{\alpha}\right)\sin\alpha\right);\\ &Y_i =\\ &= -\mu_y\left(\left(\ddot{z} - z\dot{\alpha}^2\right)\sin\alpha + \left(z\ddot{\alpha} + 2\dot{z}\dot{\alpha}\right)\cos\alpha\right);\\ &L = -mz\left(z\ddot{\alpha} + 2\dot{z}\dot{\alpha} - \ddot{x}_i\sin\alpha + \ddot{y}_i\cos\alpha\right). \end{aligned} \tag{24}$$

In a similar way as for the previous case here:

$$Z = \frac{0{,}25m\left(\omega^2 A\right)^2 \sin 2\alpha_0}{\left[\left(n_x^2 - \omega^2\right)^2 + \left(h_x\omega\right)^2\right]\left[\left(n_y^2 - \omega^2\right)^2 + \left(h_y\omega\right)^2\right]} Z_s, \tag{25}$$

where

$$\begin{aligned} &Z_s =\\ &= \left(\mu_x - \mu_y\right)\left(n_x^2 - \omega^2\right)\left(n_y^2 - \omega^2\right)\left(\omega_k - \omega^2\right) +\\ &+ \left[\mu_x\left(n_x^2 - \omega^2\right)h_y^2 - \mu_y\left(n_y^2 - \omega^2\right)h_x^2\right]\omega^2, \end{aligned} \tag{26}$$

where

$$\omega_k^2 = \frac{\mu_x n_y^2 - \mu_y n_x^2}{\mu_x - \mu_y}. \tag{27}$$

Z is the square of the eigenfrequency of the case of the exciter of vibrations α.

Stability of the dynamical stationary positions changes when the sign of Z_S passes from positive to negative and vice versa.

When the forces of friction $h_x = h_y = 0$ then Z_S changes sign when ω^2 passes through the values n_x^2, n_y^2 and ω_k^2. This is represented in Fig. 3, where stable and unstable zones at $n_x < n_y$, $\mu_x > \mu_y$ for various values of ω_k are shown.

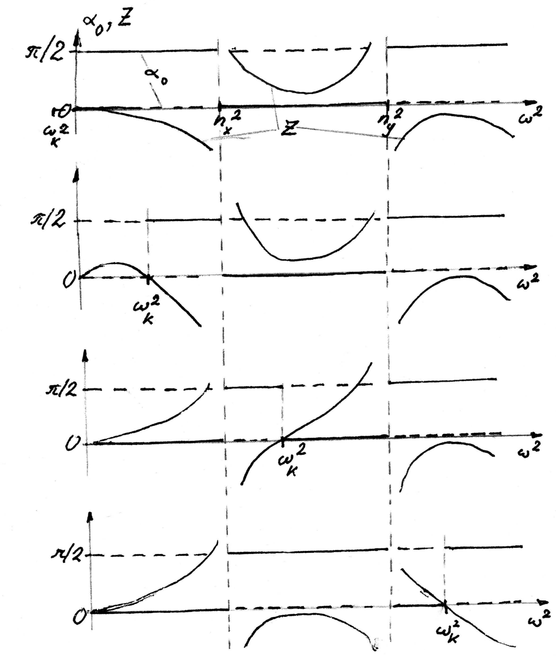

Fig. 3. Stationary zones: —— stable, - - - unstable, graphical relationships represent the square of the eigenfrequency Z of the variation of α_0 about the stationary position (positive values of Z about $\frac{\pi}{2}$ are represented in the negative direction of the vertical axis)

At small values of Z motions of chaotic type arise.

The forces of friction shift the transitional points of Z_S. If the forces of friction are small, then assuming $h_x^2 = \varepsilon h_x^2$, $h_y^2 = \varepsilon h_y^2$, where ε – a dummy small parameter, those points are sought with the help of the power series with respect to ε, for example $\omega_x^2 = n_x^2 + \varepsilon\omega_{x1} + \ldots$. Taking into account the first two members the followng is obtained:

$$\omega_x^2 = n_x^2 - h_x^2\,\frac{\mu_y}{\mu_x - \mu_y}\cdot\frac{n_x^2}{\omega_k^2 - n_x^2},$$

$$\omega_y^2 = n_y^2 + h_y^2 \frac{\mu_x}{\mu_x - \mu_y} \cdot \frac{n_y^2}{\omega_k^2 - n_y^2},$$
$$\omega_{kn}^2 = \omega_k^2 + + h_x^2 \frac{\mu_y}{\mu_x - \mu_y} \cdot \frac{n_x^2}{\omega_k^2 - n_x^2} \cdot \left(\frac{\omega_k}{n_x}\right)^2 - - h_y^2 \frac{\mu_x}{\mu_x - \mu_y} \cdot \frac{n_y^2}{\omega_k^2 - n_y^2} \cdot \left(\frac{\omega_k}{n_y}\right)^2 . \quad (28)$$

Numerical analysis of the basic system

The set of differential equations of motion in Equations (22, 23) is solved using direct time marching techniques. The results of simulation are presented in Poincare diagram in Figure 4. At every discrete value of ω time marching is continued until the transient processes cease down. Then the trajectories in phase plane $\alpha - \dot{\alpha}$ are sectioned by plane $\dot{\alpha} = 0$. It can be noted that the vibration exciter can rotate in a steady state regime of motion and thus plotting of α could be quite complicated due to possible boundlessness of α. Therefore, every value of α produced by Poincare sectioning is mapped into the interval $[-\pi, \pi]$ by simple modulus 2π transformation adding or subtracting $2\pi k$ with appropriate $k > 0$.

The amplitude of oscillation A is decreased at increasing ω to preserve constant maximum kinetic energy of the exciter (at constant α):

$$\frac{m(A\omega)^2}{2} = \text{const.} \quad (29)$$

The following parameters were selected for numerical simulation: $m = 0.1$; $m_x = 2{,}1$; $m_y = 1{,}1$; $C_x = 1$; $C_y = 1$; $h_x = 0.05$; $h_y = 0.05$. The following parameters are used: $n_x \approx 0.690$; $n_y \approx 0.954$; $\omega_x \approx 0.686$; $\omega_y \approx 0.976$.

Figure 4 shows excellent correlation between analytical and numerical analysis. In the region $0 < \omega < \omega_x$ the exciter is oscillating in the x-axis direction (angle α is zero in the steady state regime of motion). The transient process is illustrated in Figure 5 at $\omega = 0.4$.

The exciter orients itself in the direction of y-axis (angle α equal to $\pi/2$ or $-\pi/2$) in the frequency range $\omega_x < \omega < \omega_y$. The transient dynamics is illustrated in Figure 6 at $\omega = 0.7$. Chaotic system response is observed in a relatively short frequency range around $\omega = 0.75$.

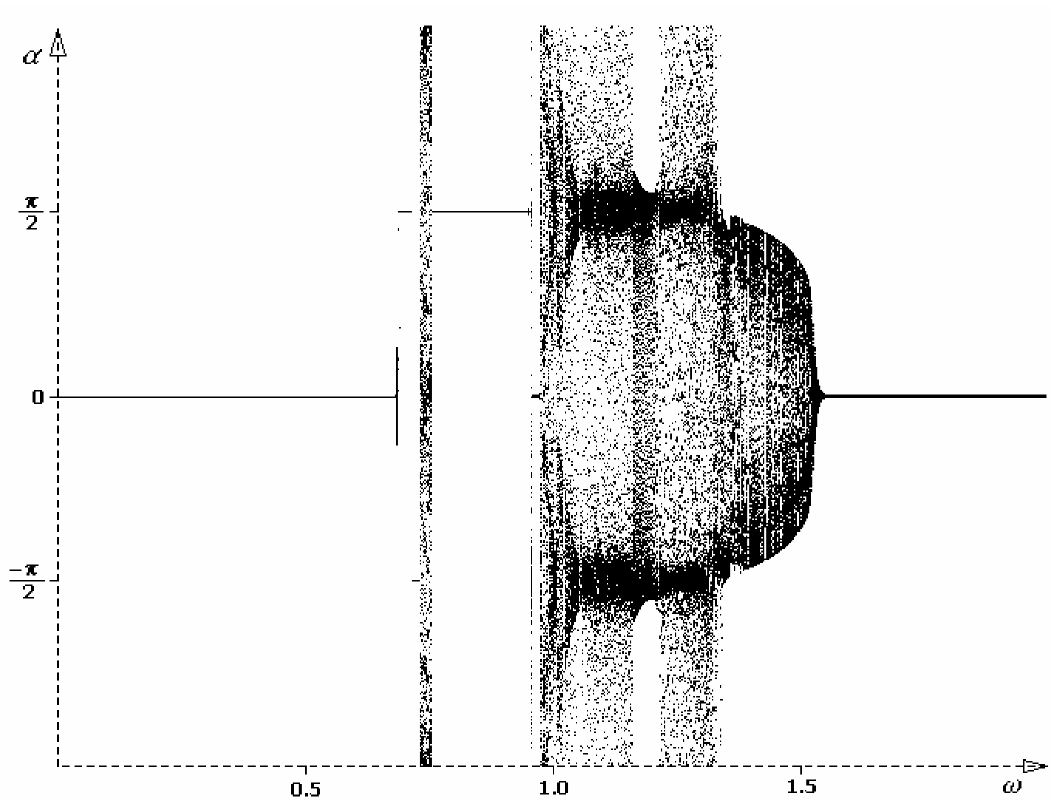

Fig. 4. Poincare map at $m = 0.1$; $m_x = 2{,}1$; $m_y = 1{,}1$; $C_x = 1$; $C_y = 1$; $H_\alpha = 0.05$; $h_x = 0.05$; $h_y = 0.05$; $A = \frac{0.15}{\omega}$

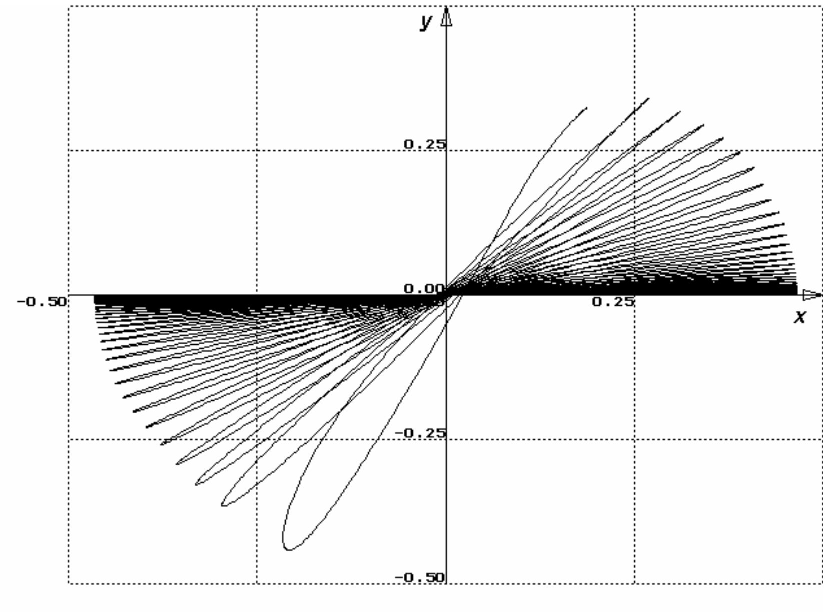

Fig. 5. Transient dynamics at $\omega = 0.4$

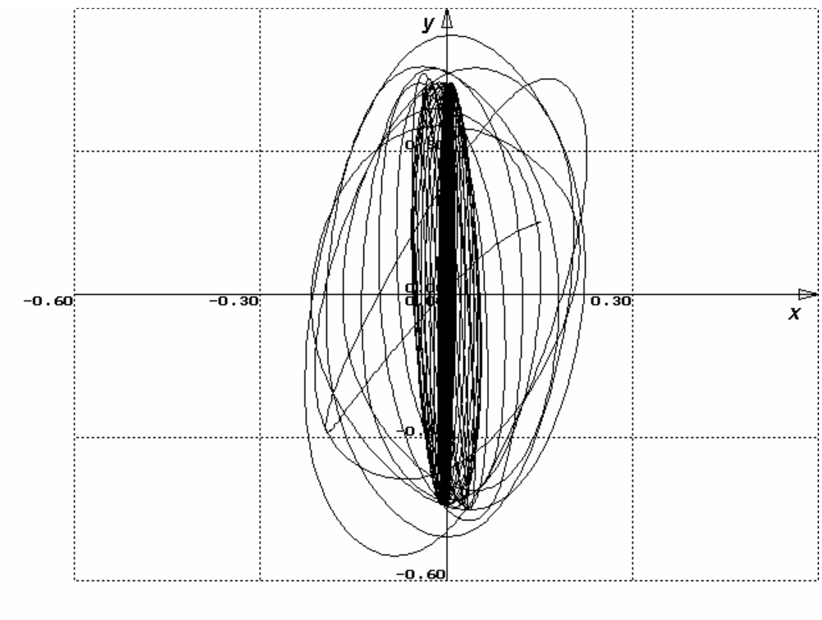

Fig. 6. Transient dynamics at $\omega = 0.7$

Finally it can be noted that the regions of chaotic response shrink at lower values of the exciter mass *m* and the amplitude *A*. But in that case the duration of the transient processes is extended, which is a quite natural result.

3. System with distributed parameters

The analyzed system is a beam, to which the cases of the exciters of vibrations which were analyzed earlier are attached by hinges.

Differential equations of motion are:

$$EF\frac{\partial^2 u}{\partial x^2} + \varsigma_x \frac{\partial u}{\partial t} - \rho F\left(\frac{\partial^2 u}{\partial t^2} + \ddot{x}_0\right) =$$

$$= \sum_j \delta\left(x - x_j\right) F_{in}\left(u_j\right)\cos\alpha_j,$$

$$EJ\frac{\partial^4 v}{\partial x^4} + \varsigma_y \frac{\partial v}{\partial t} + \rho F\frac{\partial^2 v}{\partial t^2} =$$

$$= \sum_j \delta\left(x - x_j\right) F_{in}\left(v_j\right)\sin\alpha_j,$$

$$F_{in}(u_j) = (m_0 + m)(\ddot{x}_0 + \ddot{u}_j) + \\ + m\begin{bmatrix}(\ddot{z}_j - z_j\dot{\alpha}_j^2)\cos\alpha_j - \\ -(z_j\ddot{\alpha}_j + 2\dot{z}_j\dot{\alpha}_j)\sin\alpha_j\end{bmatrix},$$

$$F_{in}(v_j) = (m_0 + m)\ddot{v}_j + \\ + m\begin{bmatrix}(\ddot{z}_j - z_j\dot{\alpha}_j^2)\sin\alpha_j + \\ +(z_j\ddot{\alpha}_j + 2\dot{z}_j\dot{\alpha}_j)\cos\alpha_j\end{bmatrix},$$

$$M_{in}(\alpha_j) = J\ddot{\alpha}_j + \\ + mz_j\begin{bmatrix}\dot{z}_j\dot{\alpha}_j + z_j\ddot{\alpha}_j - (\ddot{x}_0 + \ddot{u}_j)\sin\alpha_j + \\ + \ddot{v}_j\cos\alpha_j\end{bmatrix} + \\ + H_\alpha\dot{\alpha}_j, \quad (30)$$

$$cx_0 = EF\frac{\partial^2 u}{\partial x^2}, \quad EJ\frac{\partial^3 v}{\partial x^3} = 0, \quad EJ\frac{\partial^2 v}{\partial x^2} = 0 \quad \text{at } x = 0.$$

Analytical calculations are performed in the same way as for the systems with concentrated parameters. The values $\alpha = 0$ and $\alpha = \frac{\pi}{2}$ are obtained and this means that in the system transverse or longitudinal waves exist.

Further analysis is performed by numerical methods.

An in-plane elastic cantilevered plate is analyzed. The numerical model of the system is built meshing the continuous structure by finite element method [12]. Differential equations of motion representing the linear elastic structure are derived in the following form:

$$[M]\{\ddot{X}\} + [H]\{\dot{X}\} + [C]\{X\} = \{F\}, \quad (31)$$

where [*M*], [*H*], [*C*] – mass, damping and stiffness matrixes appropriately; $\{\ddot{X}\}, \{\dot{X}\}, \{X\}$ – global vectors of acceleration, velocity and displacement; $\{F\}$ – vector of external forces.

A vibration exciter with movable mass *m* and an additional degree of freedom (rotation) is attached to one of the nodes of the structure (black dots in Figure 7). It is clear that every node of the structure (non-cantilevered) corresponds to two degrees of freedom in Equation (31). Let's denote those two degrees of freedom corresponding to node to which the exciter is attached as *r* (corresponding to displacement in direction of *x*-axis) and *s* (corresponding to displacement in direction of *y*-axis).

Then the external forces acting to the *r*-th and *s*-th degrees of freedom will take the following form:

$$F_{in}(x) = -m\begin{pmatrix}\ddot{x}_r + (\ddot{z} - z\dot{\alpha}^2)\cos\alpha - \\ -(z\ddot{\alpha} + 2\dot{z}\dot{\alpha})\sin\alpha\end{pmatrix}; \\ F_{in}(y) = -m\begin{pmatrix}\ddot{x}_s + (\ddot{z} - z\dot{\alpha}^2)\sin\alpha + \\ +(z\ddot{\alpha} + 2\dot{z}\dot{\alpha})\cos\alpha\end{pmatrix}, \quad (32)$$

where $F_{in}(x)$ and $F_{in}(y)$ are *r*-th and *s*-th components of vector $\{F\}$. A separate differential equation describes the variation of angle α:

$$J\ddot{\alpha} + H_\alpha\dot{\alpha} = \\ = -mz(z\ddot{\alpha} + 2\dot{z}\dot{\alpha} - \ddot{x}_r\sin\alpha + \ddot{x}_s\cos\alpha). \quad (33)$$

Analysis of a continuous structure coupled with a discrete system is a computationally demanding problem, especially when one of the systems is linear and another – nonlinear [6]. The terms $m\ddot{x}_r$ and $m\ddot{x}_s$ are brought from Equation (33) to the left side of Equation (31) in order to preserve the stability of numerical time marching codes. Thus the mass matrix of the elastic structure is augmented; value *m* is added to the diagonal elements in *r* and *s* positions of the mass matrix. This augmentation naturally represents the mass increase of the node to which the vibration exciter is attached.

Initially, eigenshapes and natural frequencies of the elastic structure are calculated (with the augmented mass matrix; *m* = 0.1). The first four eigenshapes of a cantilevered plate are presented in Figure 9 where grey lines stand for the structure in the status of equilibrium; dark solid lines – for appropriate in-plane eigenshapes. Natural frequencies are printed at the bottom of appropriate eigenshapes.

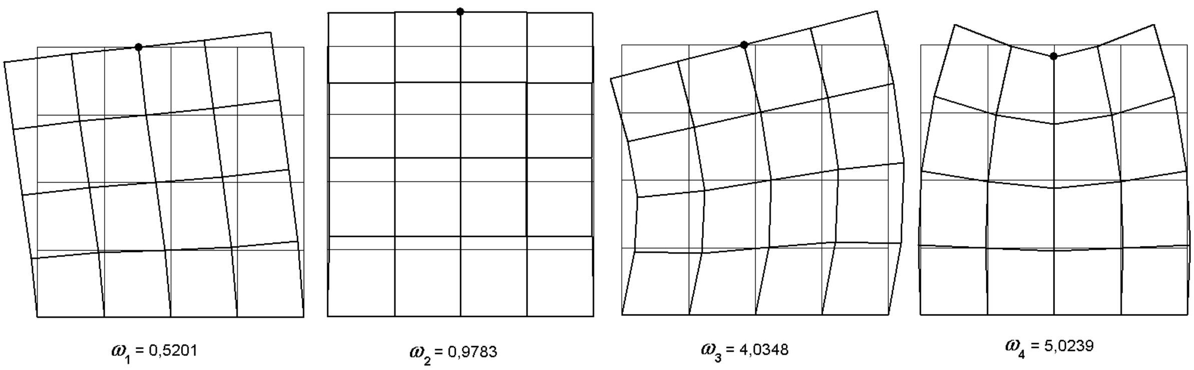

Fig. 7. The first four eigenshapes and natural frequencies of the elastic structure

Next, the transient processes are analyzed at different frequencies of excitation. In our model *r* = 23 (the degree of freedom representing the motion of the node to which the exciter is attached in the direction of the *x*-axis) and s = 24 (same node in the direction of the *y*-axis). Transient process at ω = 0.4 is presented in Figure 8; at ω = 0.65 – in Figure 9. It can be clearly seen that at ω = 0.4 angle α settles at 0, while the node to which the exciter is attached oscillates in the direction of *x*-axis (the same direction as the exciter itself). On the contrary, at ω = 0.65 angle α settles at $\pi/2$, while both the node and the exciter oscillate in the direction of *y*-axis. That is even more clearly illustrated in phase plane *x*-*y* in Figure 10 where the transient dynamics of all nodes of the structure is plotted simultaneously.

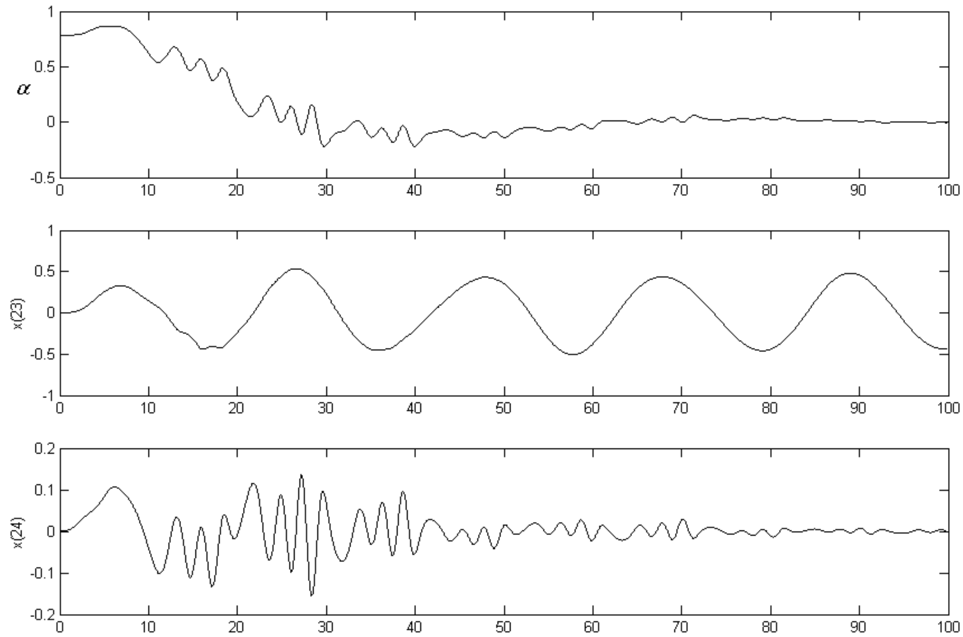

Fig. 8. α , x_r and x_s versus time – transient process at ω = 0.4

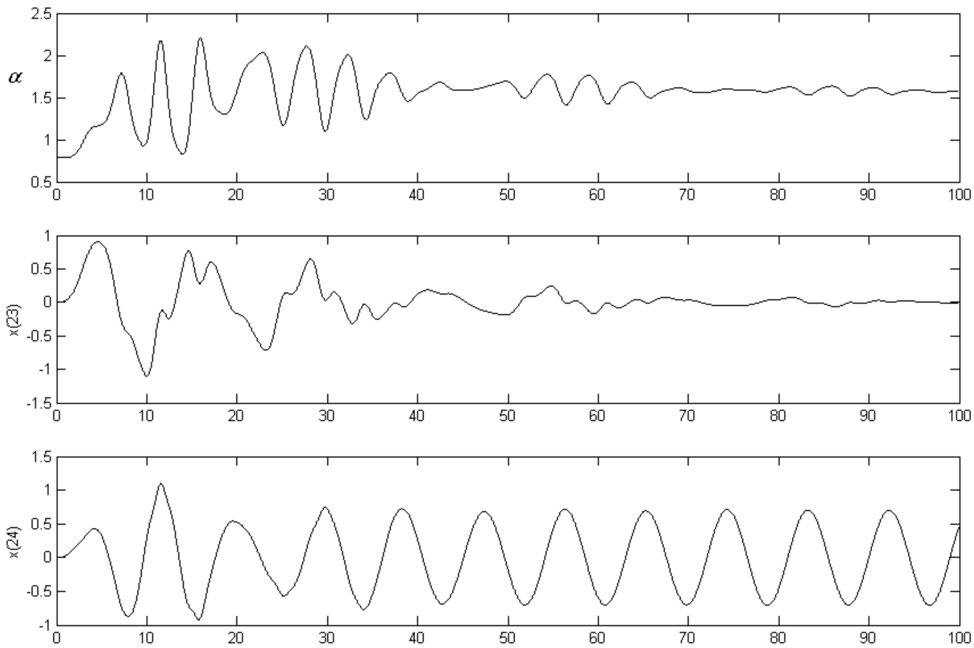

Fig. 9. α , x_r and x_s versus time – transient process at ω = 0.65

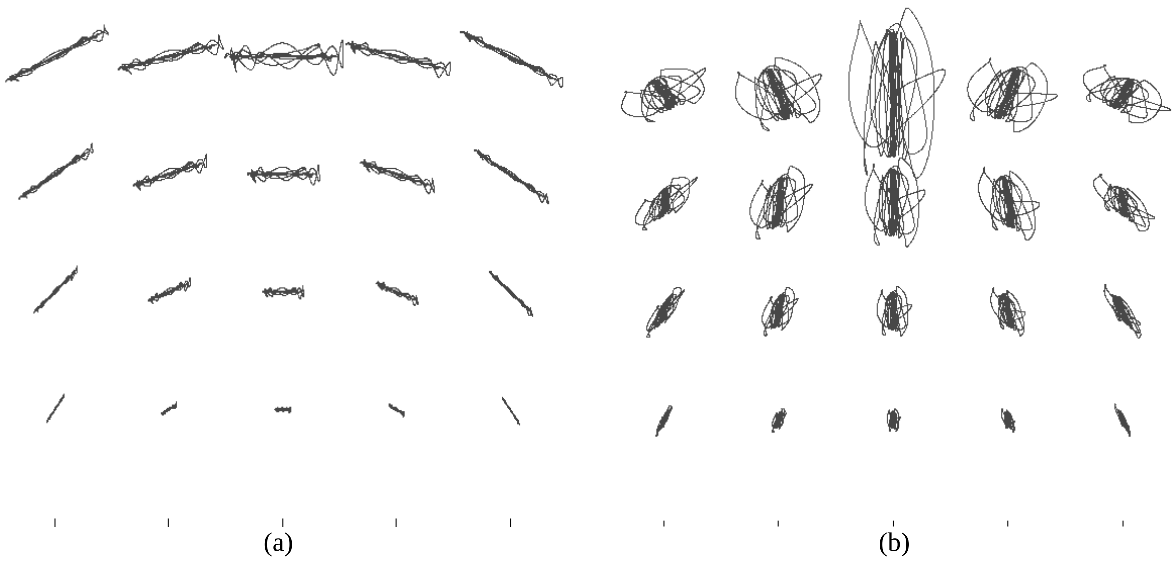

Fig. 10. Transient processes (traces of the nodes) in the phase plane at ω = 0.4 (a) and ω = 0.65 (b)

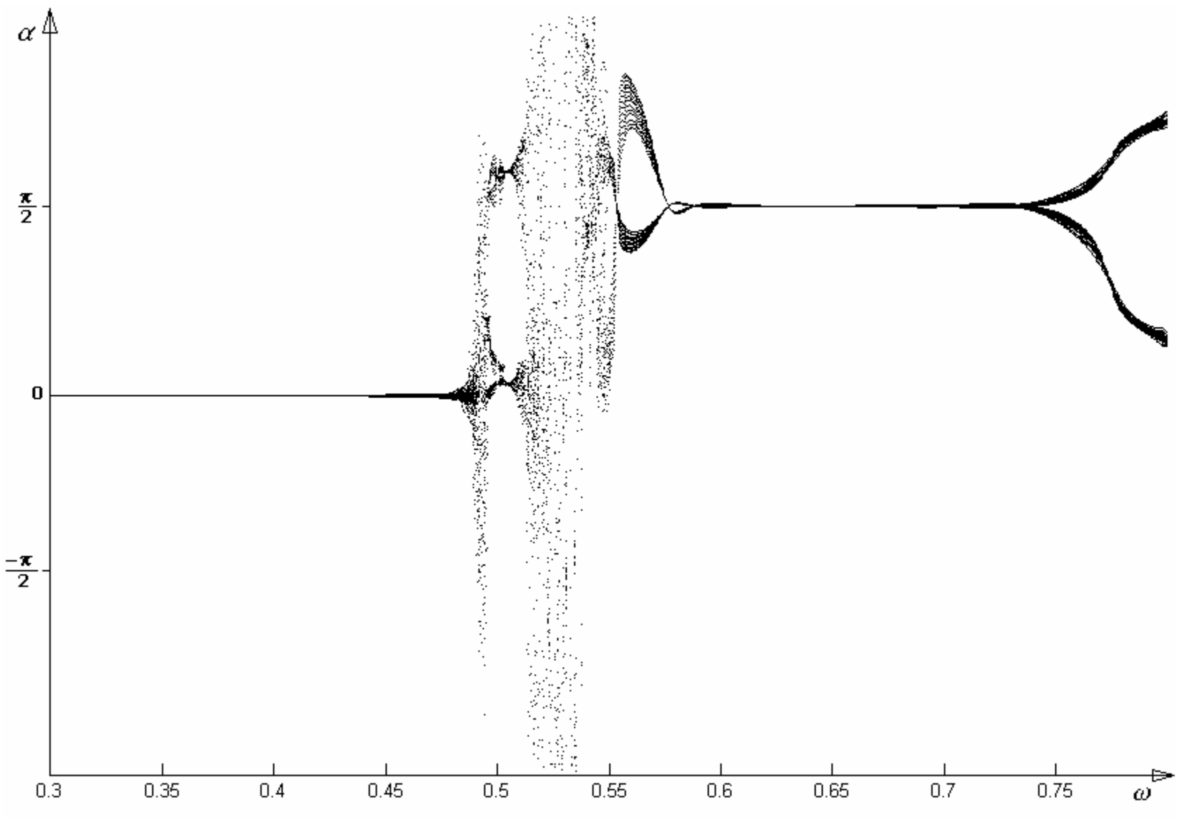

Fig. 11. Poincare map of the node to which the exciter is attached

Finally, Poincare map is constructed for steady state processes at different frequencies of excitation (Figure 11). It can be noted that the regime of motion at $\alpha = 0$ looses its stability at frequencies around 0.5. Then the process stabilizes again around $\omega = 0.6$, but already around $\alpha = \frac{\pi}{2}$.

Different nodes could be selected for attachment of the vibration exciter. General recommendation would be to select such nodes, which are most sensitive to external excitation. In our example it would be not a good idea to select a node near the motionlessly fixed nodes. In principle, the observed phenomena would be the same, but the sensitivity and the accuracy of the estimates would be considerably reduced.

Concluding remarks

The effect of self-orientation is presented and illustrated in this paper. A vibration exciter with an additional angular degree of freedom can serve as a detector of natural frequencies. Approximate analytical analysis provides insight into the principles of dynamical self-orientation and its applicability for the detection of fundamental frequencies of elastic structures. The oscillating mass and the amplitude of oscillations of the exciter must be relatively low compared to the structure under investigation in order to provide sufficiently accurate estimates.

It is determined that in the systems of analyzed type in the range of frequencies of harmonic excitation from zero up to the first critical frequency, which is equal to the partial frequency regimes of chaotic type do not exist. In higher frequency ranges of excitation there are intervals where regimes of chaotic type exist.

Only for the frequencies which are higher than the first critical frequency regimes of chaotic take place, but the average positions of motion take place about the positions calculated analytically.

References

[1] **Blekhman I. I., Fradkov A. L., Nijmeijer H., Pogromsky A. Yu.** On self – synchronization and controlled synchronization // Systems & Control Letters, 1997. V. 31. P. 299-305.

[2] **Brown R., Kosarev L.** A unifying definition of synchronization of dynamical systems // Chaos, 2000. V. 10. P. 344-349.

[3] **Ragulskis L., Ragulskis K.** Vibrating systems with the dynamical directed vibration exciter. Leningrad, Machine Building, 1987, 132 p. (Vibration Technology, Issue 11).

[4] **Trueba J. L., Baltanás J. P., Sanjuán M. A. F.** 'A generalized perturbed pendulum', Chaos, Solitons & Fractals 15(5), 2003, 911-924.

[5] **Omar H. M., Nayfeh A. H.** 'Anti-swing control of gantry and tower cranes using fuzzy and time-delayed feedback with friction compensation', Shock and Vibration 12(2), 2005, 73-90.

[6] **Belato D., Weber H. I., Balthazar J. M.** 'Using transient and steady state considerations to investigate the mechanism of loss of stability of a dynamical system', Applied Mathematics and Computation 164(2), 2005, 605-613.

[7] **Tsai C. S., Chiang T. C., Chen B. J.** 'Finite element formulations and theoretical study for variable curvature friction pendulum system', Engineering Structures 25(14), 2003, 1719-1730.

[8] **Vyas A., Bajaj A. K.** 'Dynamics of autoparametric vibration absorbers using multiple pendulums', Journal of Sound and Vibration 246(1), 2001, 115-135.

[9] **Murnal P., Sinha R.** 'Aseismic design of structure–equipment systems using variable frequency pendulum isolator', Nuclear Engineering and Design 231(2), 2004, 129-139.

[10] **Song Y., Sato H., Iwata Y., Komatsuzaki T.** 'The response of a dynamic vibration absorber system with a parametrically excited pendulum', Journal of Sound and Vibration 259(4), 2003, 747-759.

[11] **Belato D., Weber H. I., Balthazar J. M., Mook D. T.** 'Chaotic vibrations of a nonideal electro-mechanical system', International Journal of Solids and Structures 38(10-13), 2001, 1699-1706.

[12] **Bathe K. J.** Finite Element Procedures in Engineering Analysis, Prentice-Hall, Englewood Cliffs, NJ, 1982.